

An Analysis of Zambian Cast Aluminum Pots

Pinar Demetci, Michael Resnick, Mariko Thorbecke, and Anne Wilkinson
Olin College of Engineering
Needham, Massachusetts 02492

Abstract—Aluminum pots cast by Zambian small business owners often fail under normal use scenarios. Brittleness in cast Al-Si alloys may result from several factors, including large grain size and formation of intermetallic phases due to excessive impurity content. Large grains can be refined by nucleating agents such as table salt (NaCl) and provide increasing toughness. Recasting the Zambian pots with small additions of NaCl did lead to a small average increase in ultimate tensile strength and toughness across three trials, but the samples were still brittle and failed easily. This led to an analysis of fracture surfaces and failure modes. This analysis showed that the castings fail along acicular regions of excessive iron-rich contaminant. These contaminants provide easy crack propagation paths and overwhelm the benefits of nucleating agents.

Index Terms—Casting, Aluminum-Silicon Alloy, Zambian Pots, Grain Refinement, International Development

I. INTRODUCTION

Cast aluminum pots made from recycled metal are commonly used for cooking in Zambia. The pots are sand cast by small business owners that scavenge for scrap metal. The scrap metal is melted down in furnaces and recast into pots (Figure 1). Due to the varying composition of the scavenged metal and potential iron contamination from the casting crucible, the resulting alloy is brittle and these pots often structurally fail during normal use, such as being pushed along a table surface or dropped from a small height.



Fig. 1. Casting process in Zambia. Scavenged scrap aluminum is melted down in an iron crucible and stirred with an iron rod. The molten alloy is then poured into sand molds to form pots.

To reduce brittleness and increase strength in the aluminum alloy casts, a student team at Olin College of Engineering investigated a variety of approaches in spring of 2014. One of the approaches they used was reducing the eutectic grain size of the alloy since finer grain structure leads to improved mechanical properties, such as higher ultimate strength, and improved toughness [1]. To achieve this, the team tested sodium and strontium as nucleating agents. Their results indicated that sodium led to greater increases in energy absorption by the alloy upon impact [4]. NaCl is a great candidate for use in the Zambian casting process because, unlike strontium, it is readily available in Zambia and cheap.

This study analyzes the failure modes of Zambian aluminum pots and tests the hypothesis put forth by previous research that recasting a sample of a cast conglomerate of recycled aluminum-silicon alloys, with 0.003% (w/w) sodium addition would decrease brittleness. Based on these analyses, put forward recommendations around the casting process to decrease brittleness in Zambian pots.

For analyses, of five Zambian cast aluminum pots, two pots with the highest difference in their chemical composition and grain size were chosen to be used for samples. Both tensile and impact tests were performed to observe changes in overall strength since the pots being studied typically fail under dynamic loading.

II. ALLOY COMPOSITION

In order to determine the range of compositions present in a typical cast aluminum pot and lid, five different samples were sent for optical emission spectroscopy analysis. The compositional breakdown of each sample is given in Table I. Alongside this data are the recommended ranges for various common elements in the UNS A03320 alloy, which was found to be most chemically similar to the alloys studied here [6]. For comparison, a bar graph of each element (excluding aluminum) is shown in Figure 2.

| | Z0 | Z1 | Z2 | Z3 | Z4 | UNS A03320 |
|-----------|--------|--------|--------|--------|--------|------------|
| Aluminum | 83.30% | 85.70% | 87.30% | 83.40% | 86.30% | remainder |
| Silicon | 8.60% | 9.90% | 9.90% | 8.00% | 6.70% | 10.5% |
| Copper | 2.00% | 2.40% | 2.30% | 1.90% | 3.20% | 2.0-4.0% |
| Zinc | 0.70% | 2.10% | 2.10% | 2.00% | 1.80% | 1.0% max |
| Iron | 0.70% | 1.20% | 1.30% | 1.10% | 1.30% | 1.2% max |
| Nickel | 0.10% | 0.50% | 0.50% | 0.20% | 0.50% | 0.5% max |
| Magnesium | 0.30% | 0.00% | 0.00% | 0.00% | 0.30% | 0.5-1.5% |
| Manganese | 0.20% | 0.20% | 0.20% | 0.10% | 0.10% | 0.5% max |
| Other | 0.20% | 0.40% | 0.30% | 0.30% | 0.40% | 0.5% max |

TABLE I
CHEMICAL COMPOSITIONS OF THE ALUMINUM POTS FROM ZAMBIA

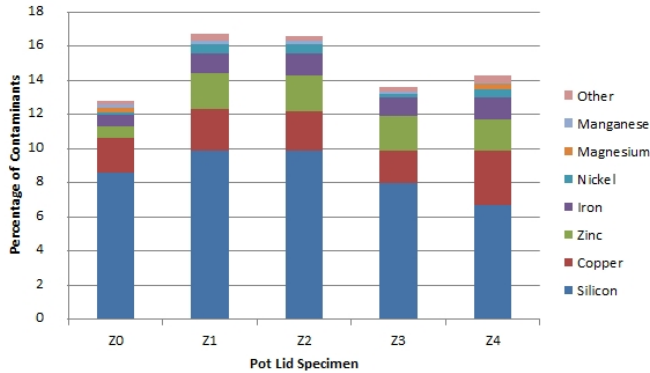


Fig. 2. Percentage of the other elements present in the five cast aluminum alloy samples displayed on a graph.

The pots exhibit a wide range of compositions, which is consistent with the unpredictability of their strength and ductility. Because of the variety of scraps used in this pot casting process, there are far more contaminants present than there are in typical Al-Si alloys, which have 2-4 alloying elements. Although several of these elements, such as silicon and copper, can improve strength, others, such as manganese, typically have a neutral effect on mechanical properties, and some contaminants, particularly iron, are widely known to increase brittleness significantly, even when in trace quantities, as supported by our research. Additionally, although many aluminum alloys use silicon percentages much higher for easier casting and higher hardness, even 0.01% (w/w) silicon is enough to substantially impact mechanical properties by dissolving in the alpha-solid solution and helping prevent dislocation motion by modifying the lattice orientation [8].

Liquid aluminium is capable of dissolving iron from unprotected steel tools and/or furnace equipment. Equilibrium Fe levels can reach 2.5 wt% in the liquid phase at normal melt temperatures of 700°C and up to 5 wt% for a melt held at 800°C [7].

Thus it may be useful to note that when using an iron-based crucible, like the one used to produce the pots being studied, using a lower melt temperature will result in less iron introduction. It is likely, however, that the melt temperature is kept as low as possible anyway to save energy.

III. EXPERIMENTAL METHODS

The efficacy of any recommendation made for toughening the alloy will vary depending on composition. Therefore, of the 5 Zambian pot samples, we used the two that had the biggest difference in grain size as well as aluminum and silicon compositions for our laboratory tests and analyses. These samples are referred to as “Z1” and “Z4”.



Fig. 3. The two pot lids chosen for experimentation. Z4 (left) and Z1 (right).

In order to compare the mechanical properties before and after addition of a nucleation agent, a 0.03% (w/w) NaCl was added to half of the samples, as recommended in ASM handbook [4].

A total of 12 impact test specimens and 12 tensile strength test specimens were cast using investment molding. Specimen geometry and dimensions are shown in Figure 4. Table salt was added to the aluminum before melting and then stirred when the aluminum melted. Boric acid powder was added to the melt in order to prevent oxidation. Prior to testing, samples were cleaned of flash and other surface imperfections from the casting process.

Impact and tensile strength tests were run on samples from both lids, cast both with and without salt. The tests were run with three specimens for each case. Instron Impact Testing System was used to apply a dynamic load of 25.9 joules to the impact samples. The samples were oriented so that the notched side would face down. The tensile strength tests were conducted on Instron Single Column Universal Testing System using a 5000 kN load cell.

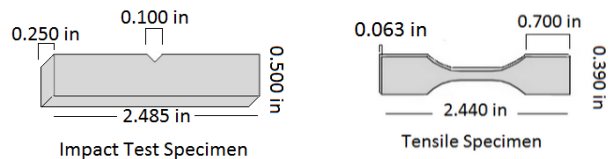


Fig. 4. Cast specimens used for mechanical testing. The impact specimen has dimensions 2.49” x 0.5” x 0.25”, with notch depth and width of 0.10”. The tensile specimen has major dimensions of 2.44” x 0.39” x 0.063”.

Microstructural analysis was performed on polished samples of Z1 and Z4, as well as on the fracture surfaces. Then, EDS was performed on the fracture surfaces in order to identify the chemical composition of each region.

IV. MICROSTRUCTURAL ANALYSIS

Microstructural analysis was performed on both NaCl modified and unmodified samples of the pot recastings. Long, acicular regions and rosette regions were identified as phases containing contaminants such as Fe and Cu, Ni, Zn, respectively. In addition, microstructures showed substantial differences in composition between Z1 and Z4. For example, in pot lid Z1, the micrograph without salt (Figure 5) contains no dendrites. This suggests that the entire sample is a eutectic solid with large grain size, where large light grey regions correspond to the aluminum-rich alpha phase, and the dark grey region is a silicon beta phase. The irregular regions are smaller eutectic grain formed by faster cooling within the localized area. Comparison to the ASM handbook micrographs suggested the light grey acicular regions were an iron-rich intermetallic compound. There are three possible candidates for the composition of the contaminant: $Fe_2Si_2Al_9$, Cu_2FeAl_7 , and Fe_3SiAl_2 . After close examination of the different microstructures formed by these solids, the $Fe_2Si_2Al_9$ solid bore the most resemblance to the acicular spikes seen [5]. Without salt, the solid aluminum regions that formed were relatively smaller and disjointed. When salt was added (Figure 6), it appeared to increase the grain size of the eutectic aluminum solid. In addition, large iron-rich spikes are present in both castings, and the salt appears to have made those acicular regions larger but fewer.

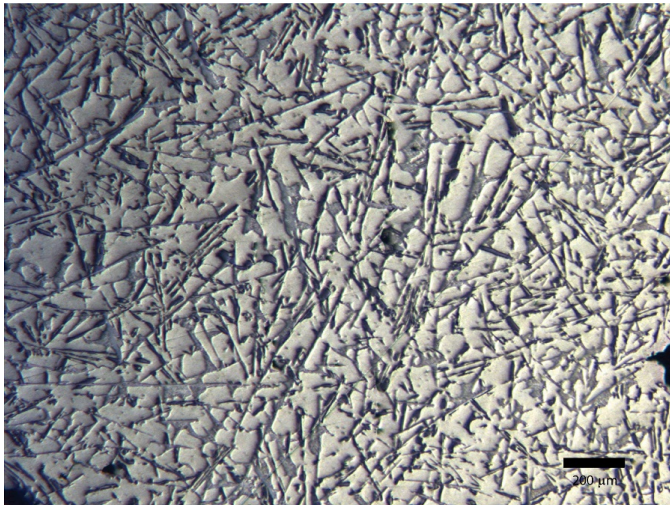


Fig. 5. Z1 without salt modification. Light grey regions are aluminum rich alpha solid, and dark grey regions are silicon beta solids. Long light grey acicular spikes are an iron-containing intermetallic impurities. The lack of alpha dendrites suggest a eutectic composition for Z1.

Z4 has a smaller overall grain size than Z1, and appears to be hypoeutectic (Figures 7 and 8). This explains the large percentage of aluminum-rich alpha solid. The alpha solid,

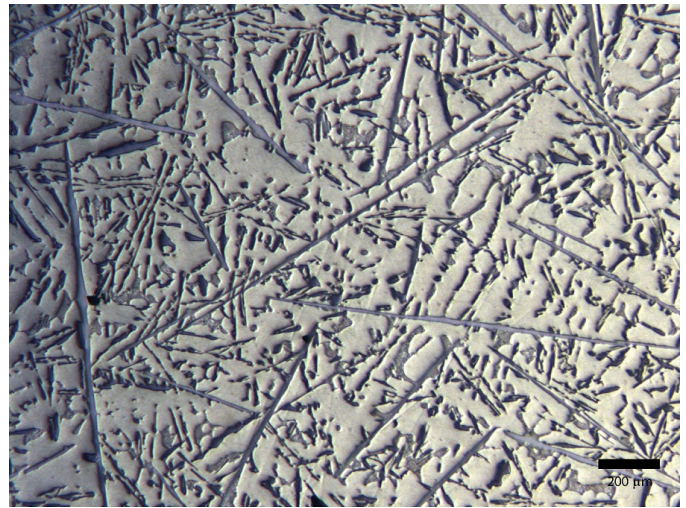


Fig. 6. Z1 with salt modification. The alpha solids became rounder at their edges. The acicular iron regions are fewer and larger in the modified Z1 sample than the original Z1 sample.

consistent with many aluminum alloys, formed a long, rounded dendritic structure. This structure is present especially in the modified sample.

In Z1, the salt resulted in a more rounded alpha solid. The iron-rich acicular regions became sparser and larger in all modified samples. The reason hypothesized is that the salt acts as a nucleating agent for the iron-based intermetallic, allowing it to form earlier and have more time to create large regions. It could also be because larger alpha dendrites forming in the modified samples could have pushed iron contaminant phases together.

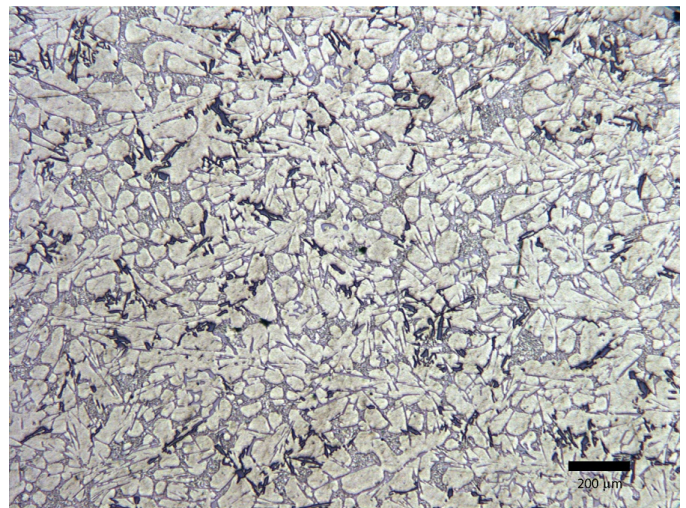


Fig. 7. Z4 without salt modification. Z4 has a much smaller grain size than Z1, and has a large concentration of alpha solid. This suggests that it is hypoeutectic. Note that the alpha phase has rounder edges.

V. FRACTOGRAPHY

Fracture surface images of the impact specimens were captured using stereo microscopy, optical microscopy, and scanning electron microscopy (SEM) in order to identify the areas of brittle fracture.

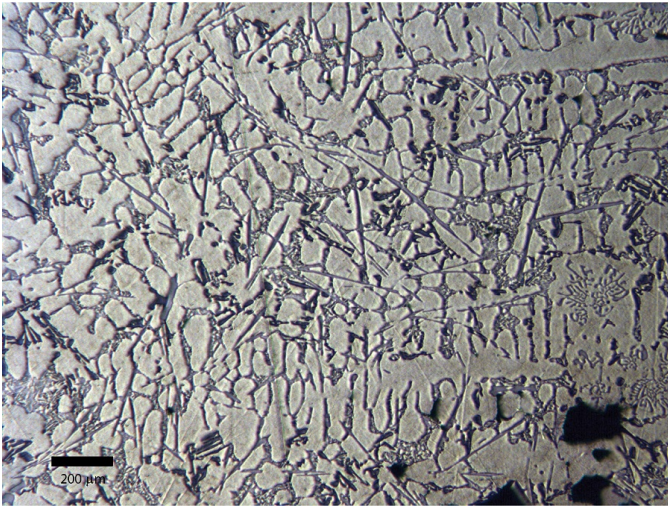


Fig. 8. Z4 with salt modification. In this sample the alpha solid formed a large dendrite structure. The iron contaminant condensed into fewer and larger spikes than in the unmodified sample.

In addition to acicular regions, an interesting structure formed by contaminants in both samples was the rosette, shown in 9. Given its shape and the fractography that follows, it appears to be a less damaging contaminant than the sharp acicular regions, and is suspected to be fairly innocuous. The rosette is likely copper, nickel and zinc. The microstructure of the “rosette” most resembles that of Cu_3NiAl_6 .

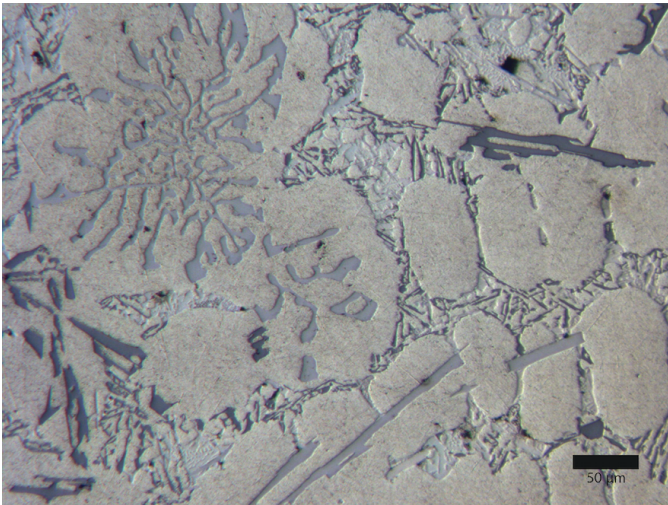


Fig. 9. The medium-grey, symmetrical region is an intermetallic impurity referred to as a “rosette”. This particular rosette is from a micrograph of a modified Z4 sample, but is present in all of the samples.

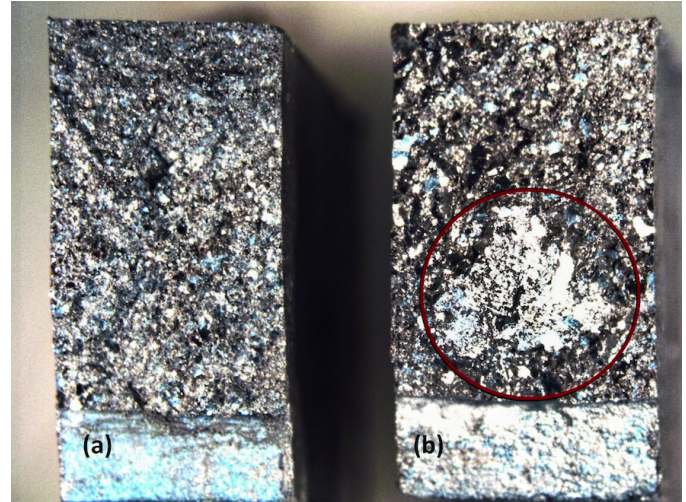


Fig. 10. Stereo microscopy images of fracture surfaces of Z4(a) and Z1(b) after the impact testing. Z4 has more fibrous surface, whereas Z1 has more flat areas. The circled flat region indicates that Z1 is more brittle than Z4.

Figure 10 is a stereo microscopy comparison of two fracture surfaces from unmodified samples of Z1 and Z4. The major difference is that Z4 has a more fibrous surface, whereas Z1 has a more planar surface. These planar surfaces are caused by perpendicular fractures, which are indicative of brittle fractures. By contrast, ductile fracture surfaces are rougher in appearance due to the plastic deformation the material undergoes. [3]

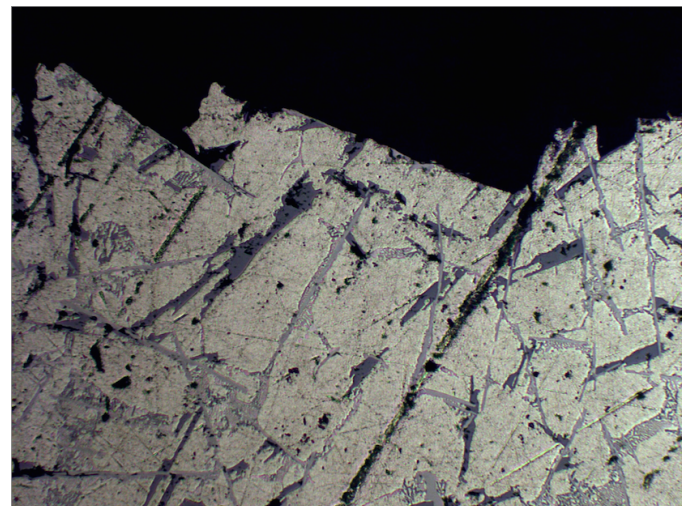


Fig. 11. Optical microscopy image of fracture surface on Z1. The crack follows the gray-colored acicular structures that are identified as iron-rich regions in EDS.

After stereo microscopy, fracture surfaces are investigated using optical microscopy. A micrograph of the Z1 fracture surface is shown in Figure 11, which shows that cracks followed an intergranular pathway. This indicates that the phase in the grain boundary that the crack traveled along, which was identified as gray-colored iron-rich acicular region, is a brittle region. [3]

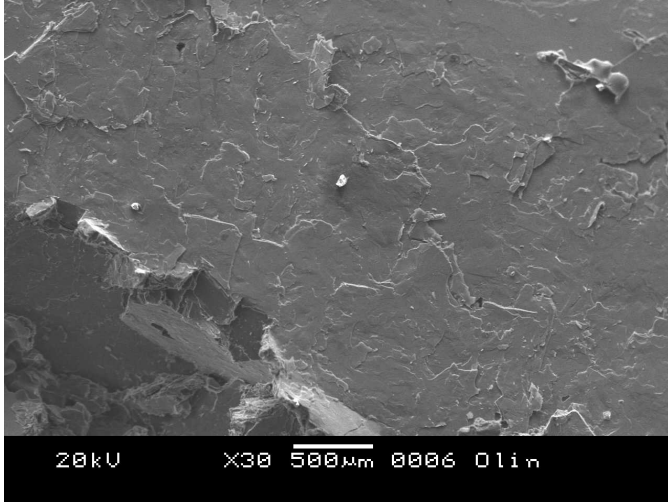


Fig. 12. SEM image of the large planar region of Z1 that was circled in Figure 10. EDS analysis confirmed that these were iron-rich regions.

An SEM image of the circled flat area from Figure 10 is given in Figure 12. Using EDS, this flat region was identified as an iron-rich region. This confirms that the acicular needle-like structures in the optical microscopy images around the intergranular fracture pathway are iron-rich plates. Additional SEM images of Z1 and Z4 are displayed in Figures 14 and 13, respectively. Z1 has more iron-rich plates, whereas Z4 has more dendrites (circled in Figure 13). The dendrites were identified as the aluminum-rich regions of the alloy in the "Microstructure" section. This is consistent with the compositions found through EDS analysis. The Z4 alloy has more dendrites due to the higher percentage of aluminum. The difference between the number of dendrites and iron plates in Z1 and Z4 might be the primary reason why one is more brittle. In general, ductile fractures are more desirable because the plastic deformation leads to slower crack propagation and more total energy absorbed upon impact.

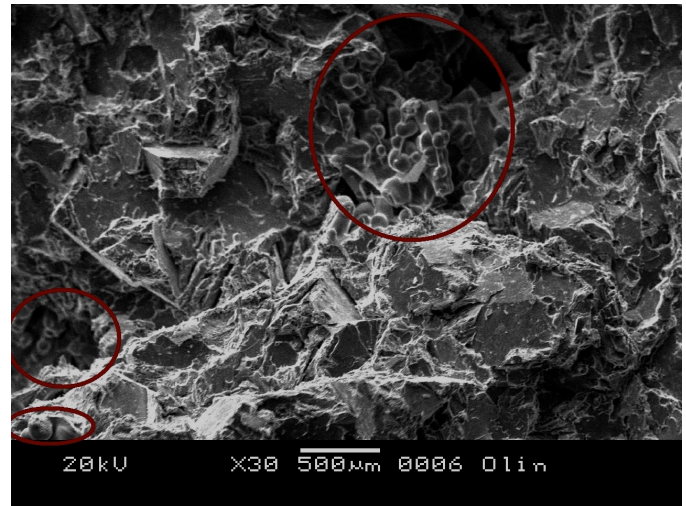


Fig. 13. SEM image of fracture surface of Z4. Circled areas show aluminum-rich dendrites that are more ductile structures in the alloy.

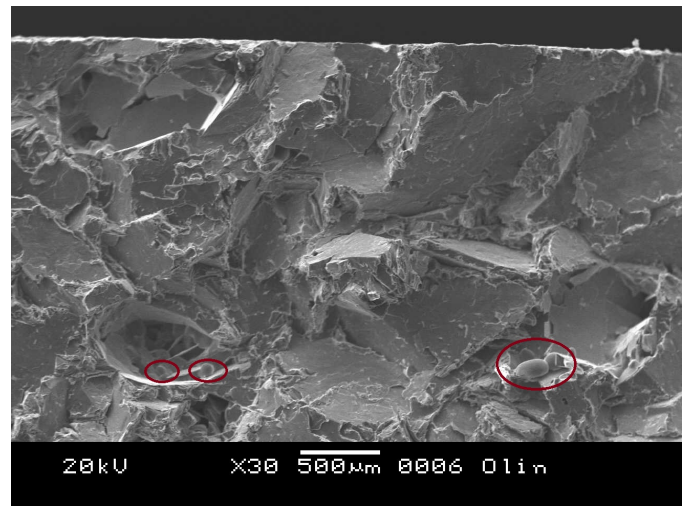


Fig. 14. SEM image of the fracture surface of Z1. Circled areas show aluminum-rich dendrites, as identified in EDS analysis. Note that there are more aluminum-rich dendrites in the SEM images of Z4, whereas there are more iron-rich flat areas in Z1. This suggests that the primary reason why Z1 is brittle is due to having less dendrites and more large iron-rich plates in its microstructure. In fact, the compositional analysis of Z4 confirmed more aluminum percentage in Z4 than in Z1 (86.30% and 85.70%, respectively).

VI. ENERGY DISPERSIVE X-RAY SPECTROSCOPY(EDS)

A. Spot Analysis

Microstructural analysis helped us identify different regions in the aluminum alloys and hypothesize compositions. Fractography enabled us to identify regions that contribute to brittleness. EDS analysis will help us confirm the composition of these structures. From the microstructure. Figure 15 is an image of an impact specimen from Z4, with six different points used for EDS analysis, corresponding to different microstructures.

The chart in Figure 16 corresponds to the energy profiles of the compounds contained in point 3, which is located on

the flat surface of a brittle fracture. From the fractography, it is clear that the alloy is undergoing brittle fractures along the flat planes of the fracture surface, and the acicular regions of the microstructure. Through microstructural analysis and comparing the acicular regions to contaminant-rich structures commonly found in aluminum alloys, $Fe_2Si_2Al_9$ was identified as the most likely composition. The large percentage of Al, Fe, and Si compositions from EDS confirms $Fe_2Si_2Al_9$ as the acicular impurity and brittle plane.

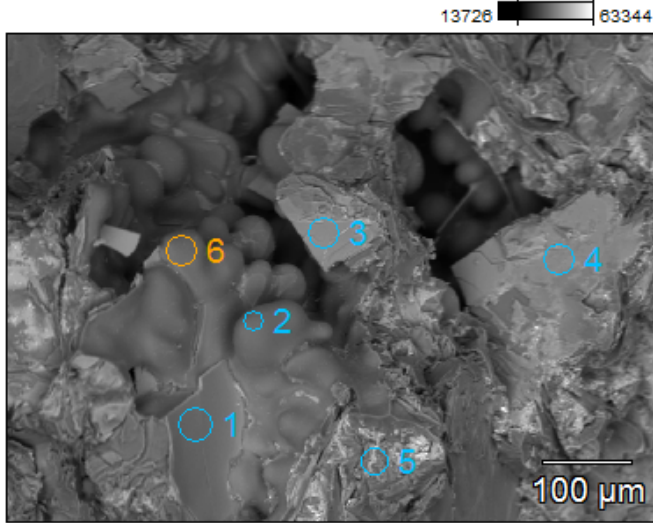


Fig. 15. Fracture surface of Z4, with six different points sampled for EDS analysis. The energy profile charts for points 3, 6, and 5 respectively are in Figures 16, 17, and 18.

The round dendritic regions were also analyzed in order to confirm their identity as aluminum alpha solid. Point 6 of Figure 15 is positioned on one of the dendrites, and its corresponding composition is shown in Figure 17. It shows that this region is almost pure aluminum.

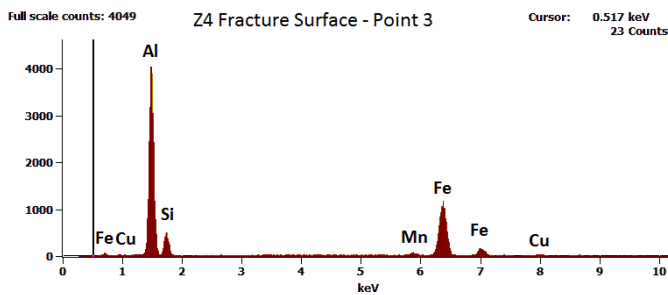


Fig. 16. Chemical composition of Point 3. Point 3 was sampled from a flat surface region. The large amount of iron supports the hypothesis that the alloy is fracturing along iron-rich regions.

In this sample of Z4, point 5 (Figure 15) was hypothesized to be a region of aluminum-silicon eutectic. According to its energy profile as depicted in Figure 15 Point 5 appears to have appropriate amounts of Al and Si to be classified as eutectic (12.2% Si, 82.8% Al).

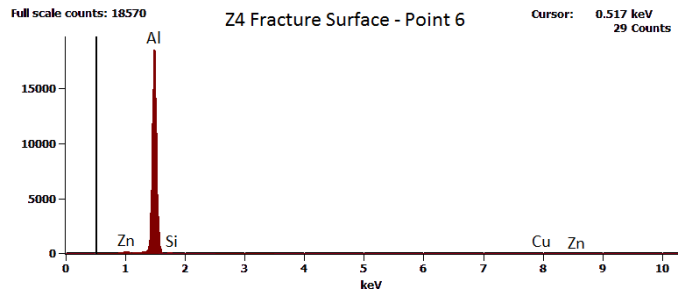


Fig. 17. Chemical composition of Point 6. Point 6 was positioned directly over an alpha dendrite.

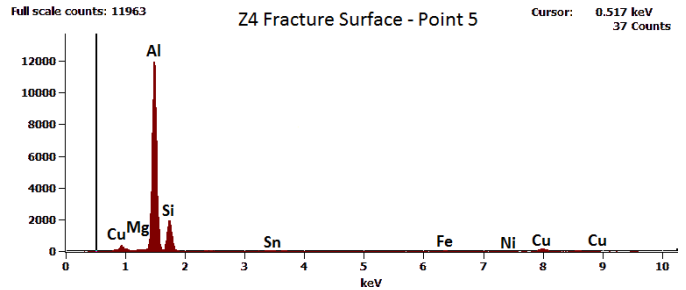


Fig. 18. Chemical Composition of Point 5. Point five was positioned over an irregular region of the fracture surface. The large amount of aluminum and smaller amount of Silicon suggest that this is part of the Al-Si eutectic.

The Z1 fracture surface (Figure 19 is also analyzed using EDS. Additionally to the structures described above, a medium grey, symmetrical impurity described in the microstructure section as a "rosette" is captured in Figure 19. Its composition is analyzed in the energy profile chart for point 3 in Figure 20.

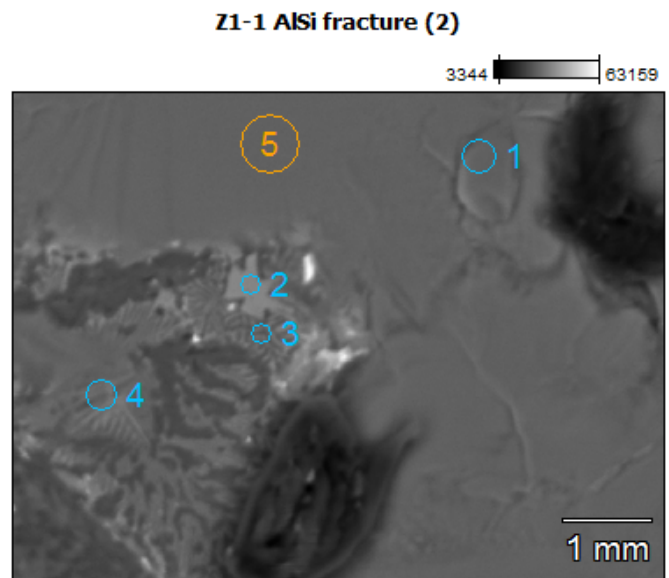


Fig. 19. Fracture surface of Z1, with five different points sampled for EDS analysis. The energy chart for point 3 is given in Figure 20

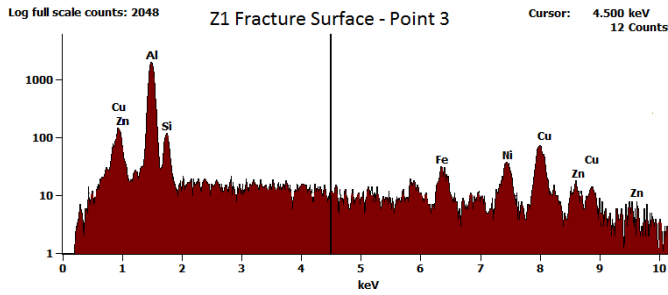


Fig. 20. Chemical composition of Point 3. Point 3 was sampled from a symmetrical, light-grey “rosette” region of impurities. The results display a large number of different compositions. The rosettes are likely where many of the Cu, Ni, and Zn impurities are present.

The “rosette” has a large mix of Cu, Ni, and Zn. By examining microstructures, Cu_3NiAl_6 was hypothesized to be the primary component. There is copper, aluminum, and nickel present in this area but there are some other elements such as zinc or iron which are unaccounted for.

Both Z1 and Z4 samples had similar characteristics although in different quantities. Points samples from flat surfaces in both specimens had a high concentration of iron, whereas, more ductile fracture surfaces had higher concentrations of aluminum.

VII. MECHANICAL PROPERTY ANALYSIS

The objective of adding salt to the castings was to offer the alpha solid extra nucleation sites so that more solids of smaller size would form. The grain-refining process generally helps to increase the energy needed for crack propagation, and so it is expected to increase toughness and strength. In order to test the effects of salt addition, we ran two tests: impact and tensile strength tests, as explained in the Experimental Methods section.

A. Impact Testing

The bars on Figure 21 display the average energy absorption for each set of tests. The results show that original Z4 samples absorbed 48.27% more energy than original Z1 samples on average (0.76 J and 0.51 J, respectively). Overall, the Z4 samples were less brittle and took more time to fracture, leading to higher energy absorptions. The optical microscopy images for Z4 show larger primary aluminum dendrites compared to Z1. These dendrites are soft and ductile. Thus, they help absorb more energy via plastic flow. Additionally, the large number of acicular iron-rich contaminants in Z1 provide an easy path for crack propagation without any dislocation motion. Finally, Z4 samples had finer eutectic grains than Z1. Finer grains require a propagating crack to change directions more frequently, resulting in more energy needed to continue propagation.

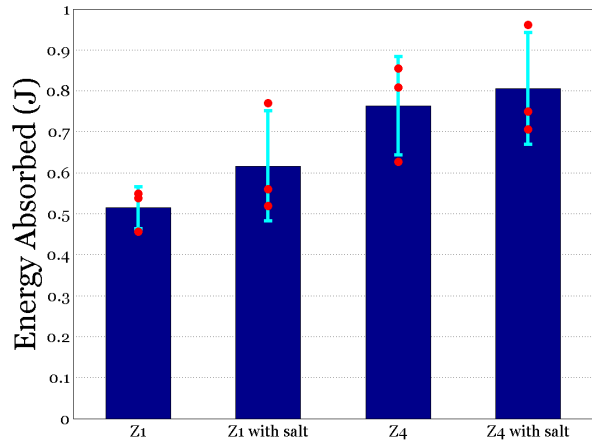


Fig. 21. Energy absorption during impact with standard deviation bars. Overall, Z4 performed better than Z1. There was also a marginal increase in energy absorption in the modified samples.

Salt addition increased energy absorption throughout impact on average. Z1 samples with salt addition absorbed 19.82% more energy than Z1 original samples did on average (0.62 J and 0.51 J, respectively). Z4 samples with salt addition absorbed 5.58% more energy than Z4 original samples on average as well (0.81 J and 0.76 J, respectively). The smooth dendritic alpha regions present in the NaCl samples lends a more ductile structure. However, the iron-rich acicular phases are also fewer but longer in the NaCl samples, allowing for easier crack propagation. This has the potential to overwhelm the potential benefits of the ductile alpha dendrites since most fracture surfaces would be most likely to occur along the iron spikes, as shown in optical microscopy.

The mean of energy absorption results suggest an increase in the impact toughness of the alloy with the addition of NaCl. However, the large overlap between the standard deviation bars demonstrate the variation between results for each individual sample. In order to validate the effect of NaCl addition on impact toughness, more tests would need to be run with a larger sample size.

B. Tensile Strength

Increases in average tensile strength were observed after addition of NaCl in both Z1 and Z4 (Figure 22). The variance in strength values make it difficult to make a strong conclusion about the effect of salt addition on tensile strength. The confidence interval for the modified Z4 trials, however, has no overlap with that of the Z4 original trials, providing evidence that salt addition may increase the ultimate tensile strength of the Z4 sample on average. It is suspected that the same would be true of Z1 given the corroborating impact data, and that the large variance in measured strength is a consequence of its relatively high brittleness.

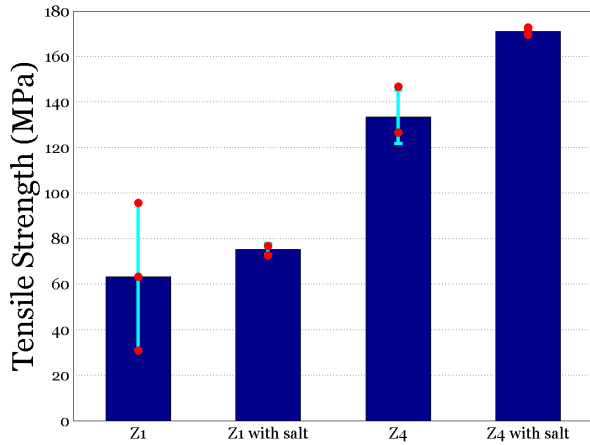


Fig. 22. Tensile yield strength. Once more, Z4 performed much better than Z1. There was also a marginal increase in yield strength with the addition of salt.

Original Z4 was observed to have higher strength than original Z1, which was expected since it has larger alpha dendrite structures and a finer eutectic region. Z1's strength increase with salt addition may be due to the presence of alpha regions. Z4's strength increase with salt addition may also be due to larger alpha dendrite structures than were present in the original Z4 sample.

An interesting result was that the data from the modified samples had lower variance compared to the unmodified samples. Thus, adding salt to the melt could result in a more reliable product for Zambian pot casters.

Despite the mechanical property advantages described that resulted from salt addition, however, due to elongation in the iron-rich acicular regions, at this time, there is no complete explanation for the potential toughness and strength increases of these alloys with salt addition. It is unclear as to whether adding salt would be helpful for every pot composition, as it is expected that in some cases the acicular regions would grow large enough to overwhelm the potential benefits of salt addition on dendritic regions.

C. Sources of Error

1) *Casting*: During casting, melting time in the induction furnace was consistent for the majority of samples, however, there were small variations in heating times between some castings. This could affect temperature, and, consequently, cooling time, which could impact grain sizes; cooling rate increases result in less time for grain nucleation, and thus larger grains. Because we waited 8 minutes after casting to quench, however, we expect this error to be minimal. The time spent and thus efficacy of mixing the molten aluminum with salt was also likely variable.

2) *Tensile testing*: The jaws holding the tensile specimens were, not completely parallel with one another, resulting in a few degrees of torsion when clamping samples. As the

weaker specimens would have been more affected by this prestressing, it is possible that larger strength differences between stronger and weaker specimens were reported than the actual difference.

3) *Impact testing*: The standard deviation bars for the impact testing results were overall larger than the ones in tensile strength testing results. One reason for such deviation might be the uncertainty with positioning the samples. The notches in the impact testing samples assisted the fracturing, however, they needed to be centered in the test set-up so that the notches would line up with the impact fixture. There might have been random parallax error if the positioning were slightly off. Additionally, some specimens' notches exhibited observable differences from others, such as shallower notch valleys and notch valleys with bumps, which could create stress concentrations. Repeating the test with a larger sample size would also help increase the accuracy.

VIII. CONCLUSION

Based on the results of the compositional analysis, all five original pot samples (Z0-Z4) had different chemical compositions. Mechanical testing was done on two of the five pots (Z1 and Z4) and this difference in composition had a major impact in test performance. Tensile strength and impact tests showed that Z4 performed better overall than Z1. In impact testing, Z4 original samples absorbed 48% more energy than Z1 original samples on average. Z4 samples also had twice as much ultimate tensile strength than Z1 on average. This may have been due to the increased alpha solid in Z4.

Addition of NaCl to both samples increased the energy absorption, indicating a decrease in brittleness. Tensile strength on average was also improved by the addition of NaCl. Z4 and Z1 samples absorbed 20% and 6% more energy, respectively, with the addition of salt. They also had respectively 19% and 28% higher tensile strength measurements when NaCl was added. However, due to variation between the results of individual samples, more testing needs to be done to improve confidence in these results.

Impurities in the alloys were found to be the most important issue. They provide an easy path for cracks to propagate. Even though the addition of salt enlarged the aluminum-rich dendrites, impurities contributed to decreased performance in both samples. EDS analysis showed that dendritic regions were almost pure aluminum, that flat regions were iron-rich, and that the rosette formations were a combination of copper and nickel, although the copper and nickel impurities are not the major causes of the alloys' brittleness.

The inconsistency in composition of the pots makes it difficult to make predictions regarding how salt addition will affect brittleness of a cast pot. While the addition of sodium enlarged the aluminum-rich dendrites, the contaminants played a big role in negating these effects. Even with the increases in strength, however, Z1 only increased from 63 to 75 MPa and Z4 from 133 to 171 MPa. Given that these are cast aluminum-silicon alloys, the expected value ranges from 131 MPa to 248 MPa, putting even the strongest of the alloys tested on the

weaker end of the spectrum [6]. Eliminating impurities, which result in high brittleness may be more effective than attempting to modify the alpha grain size. As such, casters should be more informed about the materials they are melting, as even trace amounts of iron can be devastating for the mechanical properties of cast aluminum-silicon alloys. Thus, if possible, the crucible used and ladle used for pouring should be coated, perhaps in a clay, since they are made of steel. Ideally, these items would not be iron-based.

It is recommended that alloys with low silicon content are chosen for the Zambian casting process to decrease brittleness. Such alloys can be found in "... applications where good casting characteristics, good weldability, pressure tightness, and moderate strength are required," such as "Ornamental grills, reflectors, general-purpose castings, automotive cylinder heads, internal combustion engine crankcases, piano plates, aircraft supercharger covers, fuel-pump bodies, air-compressor pistons, liquid-cooled cylinder heads, liquid-cooled aircraft engine crankcases, water jackets, and blower housings." Copper and zinc addition may decrease ductility, depending on the alloy, so copper or brass should not be added into the casting if possible. Also to reduce brittleness of the casting, alloys used in "automotive and diesel pistons, pulleys, sheaves, and other applications where good high-temperature strength, low coefficient of thermal expansion, and good resistance to wear are required" typically have higher silicon content, and should therefore be avoided. Furthermore, these alloys may also contain nickel, whose presence can decrease ductility and resistance to corrosion in many alloys of lower silicon content [11] p. 152–177.

IX. FUTURE WORK

"Additions of Mn, Cr, Cu, V, Mo, and W [act as morphological agents,] promot[ing] a body-centred cubic structure..." in Al-Si alloys instead of the platelet/acicular structure that is typical of Al-Si-Fe alloys [10]. In *Aluminum: Properties and Physical Metallurgy*, adding a 0.5% weight fraction of Mn to an Al-Si-14% alloy with 1% Fe was shown to result in an ultimate tensile strength (UTS) of 174 MPa, which is 1.3 times higher than the original Z4 sample's UTS, and 2.8 times higher than Z1's. Even with a 2% Fe weight fraction in a different, Al-Si-17% sample, the addition of 0.52% Mn brought the UTS up to 161 MPa [9] (p. 232). Future work could therefore involve investigating an optimal addition of manganese for these pots and whether manganese is available to the Zambian casters cheaply enough.

Further work can be done to improve the Zambian casting setup studied. Redesign of the crucible could involve safety features in addition to a change in material or lining to prevent iron dissolution in castings. Perhaps the mold can be modified to produce a sturdier design or provide more bracing in the current design.

ACKNOWLEDGMENT

The authors would like to thank Benjamin Linder for providing the Zambian pot lids for testing, Jonathan Stolk and

Matthew Neal for their technical support in the project, and Daniel Stolk of Metallurgical Engineering Services, Inc. for optical emission spectroscopy analysis of the aluminum alloy compositions.

REFERENCES

- [1] Murty, B. S., Kori S. A., Chakraborty, M. "Grain Refinement of Aluminium and Its Alloys by Heterogeneous Nucleation and Alloying." *International Materials Reviews* 47.1 (2002): 3-29. Web.
- [2] Hatch, J. E. "Aluminum: Properties and Physical Metallurgy". ASM International (1984). Print.
- [3] Hatch, John E. "Fractography". ASM International, 1984. Volume: 12. Print.
- [4] Dziallas, S., Little, L., McConnell, J., Perera, J., Rowley, B. "Zambian Pot". Olin College (2014).
- [5] Mehl, Robert F. "Metals Handbook". 5th ed. Vol. 7. Metals Park, Ohio: American Society for Metals (1972). 256-60. Print.
- [6] ASM International. "Standard Specification for Aluminum-Alloy Sand Castings", ASTM B26/B26M 05. Web.
- [7] Taylor, J. A. "Iron-containing Intermetallic Phases in Al-Si Based Casting Alloys." *Science Direct* 1 (2012): 19-33. Elsevier. Web.
- [8] ASM International. "Introduction to Aluminum-Silicon Casting Alloys." ASM (2004). Web.
- [9] Belov, N. A., Aksenov A. A., Eskin D. G. "Iron in Aluminium Alloys: Impurity and Alloying Element". London: Taylor Francis (2002). Print
- [10] Cao, X., Campbell, J. "Morphology of B-Al₅FeSi Phase in Al-Si Cast Alloys." *Materials Transactions* 47.5 (2006): 1. The Japan Institute of Metals and Materials. Web.
- [11] Kearney, A.L. "Properties of Cast Aluminum Alloys, Properties and Selection: Nonferrous Alloys and Special-Purpose Materials". Vol 2. ASM Handbook. ASM International (1990).